

Document downloaded from:

<http://hdl.handle.net/10251/81433>

This paper must be cited as:

Abdolpour, H.; Garzón-Roca, J.; Escusa, G.; Sena-Cruz, JM.; Barros, JA.; Valente, IB. (2016). Development of a composite prototype with GFRP profiles and sandwich panels used as a floor module of an emergency house. *Composite Structures*. 153:81-95. doi:10.1016/j.compstruct.2016.05.069.



The final publication is available at

<https://doi.org/10.1016/j.compstruct.2016.05.069>

Copyright Elsevier

Additional Information

Experimental assessment of a composite prototype made of GFRP profiles and sandwich panels to be used as a floor module of an emergency house

Hassan Abdolpour^{a,1}, Julio Garzón-Roca^b, Gonçalo Escusa^a,
José M. Sena-Cruz^a, Joaquim A.O. Barros^a, Isabel B. Valente^a

^a ISISE, University of Minho, Guimarães, Portugal

^b Department of Geological and Geotechnical Engineering, Universitat Politècnica de València, Valencia, Spain

Abstract

A series of experimental tests carried out on a composite prototype to be used as a floor module of an emergency house is presented in this paper. The prototype comprises a frame structure formed by GFRP pultruded profiles, and two sandwich panels constituted by GFRP skins and a polyurethane foam core that configures the floor slab. The present work is part of the project “ClickHouse – Development of a prefabricated emergency house prototype made of composites materials” and investigates the feasibility of the assemblage process of the prototype and performance to support load conditions typical of residential houses. Furthermore, sandwich panels are also independently tested, analysing their flexural response, failure mechanisms and creep behaviour. Obtained results confirm the good performance of the prototype to be used as floor module of an emergency housing, with a good mechanical behaviour and the capacity of being transported to the disaster areas in the form of various low weight segments, and rapidly installed. Additionally, finite element simulations were carried out to assess the stress distributions in the prototype components and to evaluate the global behaviour and load transfer mechanism of the connections.

Keywords: emergency house; composite materials; GFRP pultruded profiles; sandwich panels; GFRP skins; PU foam core.

¹ Corresponding author.

E-mail address: Hassan.abdolpour@gmail.com (H. Abdolpour)

1. INTRODUCTION

Typically, after a natural disaster, the surviving communities are accommodated in temporary dwellings for recovery [1]. Availability of temporary housing is crucial since it allows people to quickly commence their daily activities such as school, working and cooking [1–3]. In the field of temporary houses design, one of the critical aspects is the use materials with high functional properties and low price. Different types of temporary houses are currently available, most of which are made of steel, wood and plastics [4–6]; however, many of these temporary dwellings do not offer a basic level of security and protection for its occupants, and/or result in very complex and expensive solutions. As an alternative to the classical materials, the use of composite sandwich panels for configuring the enclosure surfaces of the house, and glass fibre reinforced polymers (GFRP) pultruded profiles for forming the main structural elements (beams and columns) present a series of advantages, being also at the same time able to fulfil any requirements.

It is interesting to note that building industrialisation through prefabrication lead to a reduction in the cost of buildings and to the improvement of the manufacturing quality [7–9]. Moreover, after a natural disaster, accessibility to the roads is limited, so low weight of the prefabricated dwellings components is a very convenient requisite for their transport [10]. The composite solution herein proposed uses GFRP profiles and sandwich panels and fits very well into this trend, as it is capable of being prefabricated, transported to the disaster area and easily assembled. Likewise, pultruded GFRP composite profiles show a series of promising advantages such as low production costs, low maintenance, high durability and immunity to corrosion and high strength [11–14]. Recently, sandwich panels have been increasingly used in structural applications due to some main features such as its high strength and stiffness to weight ratio, its immunity to corrosion, and a low thermal and acoustic conductivity [15–19]. In the past, efficiency of using sandwich panels has been proved in several structural applications such as cladding [20], facades [21,22], roofing [23] and walls [24].

In this paper, a floor residential module prototype of $2.64 \times 2.64 \text{ m}^2$ is introduced, composed of GFRP profiles and sandwich panels of GFRP skins and a polyurethane (PU) foam core. An experimental programme is conducted to evaluate the performance of this prototype, designed to support serviceability and ultimate load conditions of residential houses. Additionally, sandwich panels are tested in four-point and three-point bending tests to analyse their flexural behaviour. Furthermore, failure mechanisms and long-term behaviour (creep) are also investigated on small scale specimens obtained from cutting the original panels. Finally, in order to better understand the behaviour of the floor residential module prototype, finite element simulations were performed. This numerical modelling was also used to perform a parametric study.

This study was undertaken within the project “ClickHouse – Development of a prefabricated emergency house prototype made of composites materials” that aims to develop a prefabricated house using composite materials to be used as an emergency dwelling in disaster areas, or just as a temporary building, taking into account the necessity of providing dignified standard of living, including fundamental facilities like water, electricity and sewage to dislocated people.

2. PROTOTYPE DESCRIPTION

2.1 Concept and geometry

The proposed prefabricated modular prototype is schematically represented in Fig. 1. In this stage of the study, for the sake of simplicity, effects of roof and walls were not taken into account. Thus, the study will be mainly focused on the floor slabs.

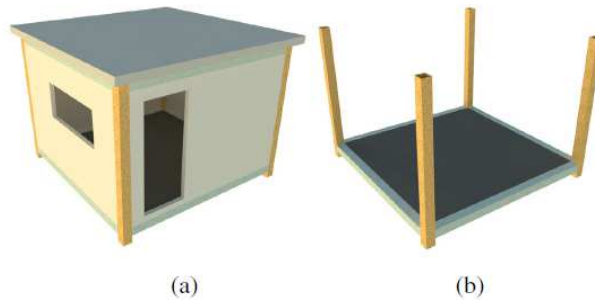


Fig. 1. Schematic of the modular prototype: (a) full prototype; (b) prototype without walls and roof.

The modular building floor prototype is comprised of two main components: the frame structure (columns and beams) and the slab that is composed of two sandwich panels. The sandwich panel contains an interior polyurethane (PU) foam core enclosed by two GFRP skins. The core and the skins have different functions: while skins bear the bending loads, the core deals with the shear loads, stabilises the skins against buckling and wrinkling, and provides thermal and acoustic isolation.

Fig. 2 shows the frame structure of the prototype, which is constituted by four GFRP beams supported in four short columns. Tubular GFRP pultruded short elements with cross section of $120 \times 120 \text{ mm}^2$ and a wall thickness of 8 mm are used as columns; for the sake of decreasing segments variation in the manufacturing process, the same profile was used for the perimetral beams. In Fig. 3, a schematic view of the two floor sandwich panels is depicted. Sandwich panels presented an overall height of 70 mm, a width of 1200 mm and a length of 2400 mm. On the contour of the panel a GFRP pultruded profile (U60 x 55 x 5) was adhesively bonded for its easy connection to the supporting elements (see Fig. 3 – section CC).

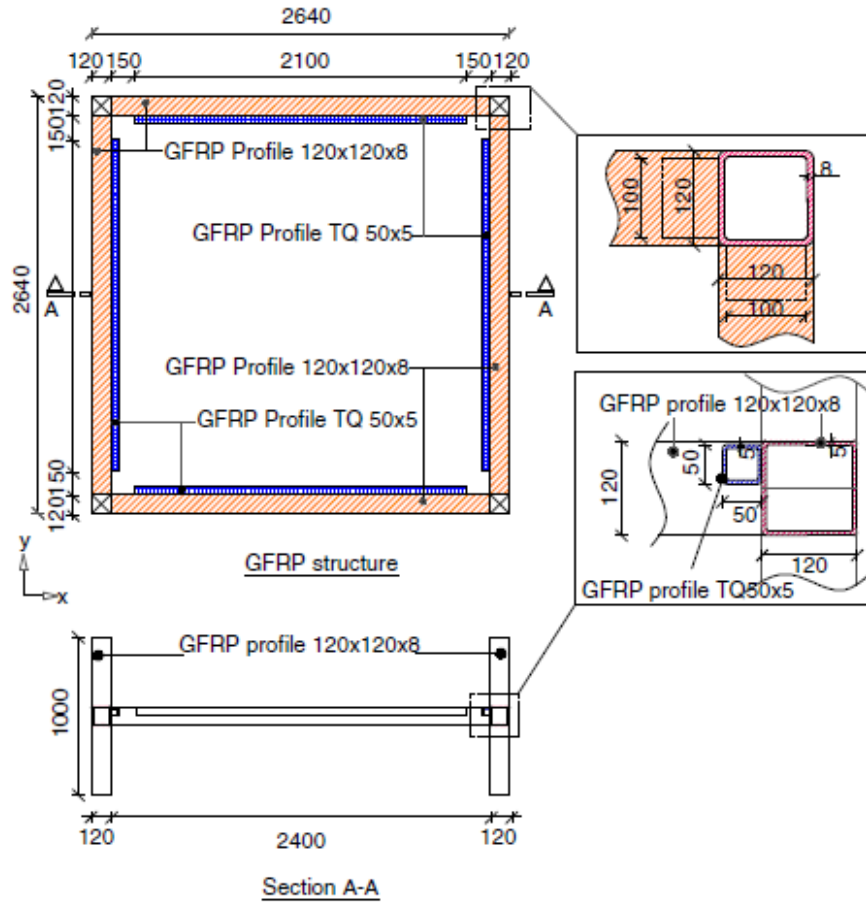


Fig. 2. Prototype frame structure (all units in millimetres).

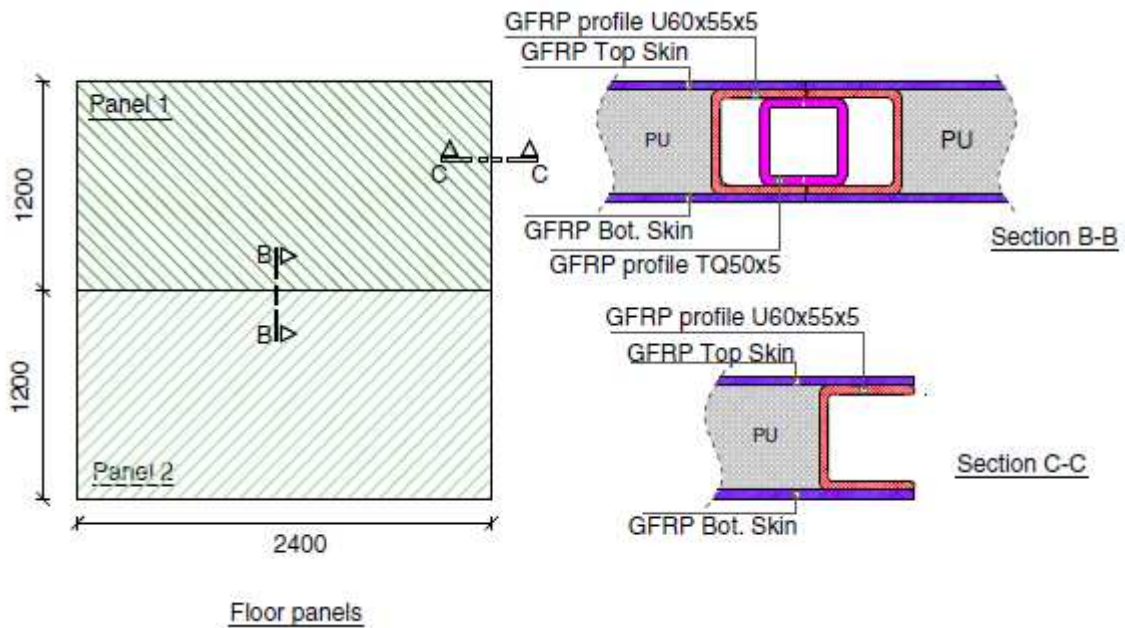


Fig. 3. Sandwich floor panel description (all units in millimetre).

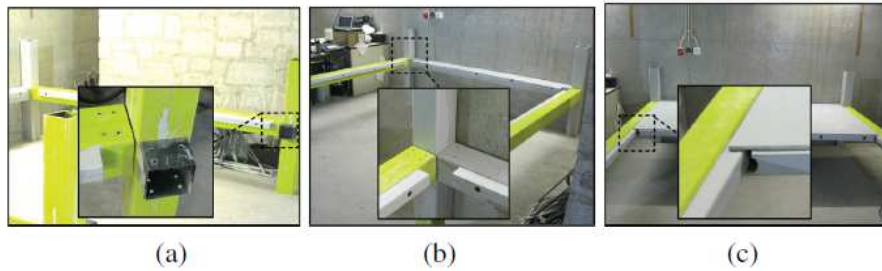


Fig. 4. Connections details: (a) beam–column; (b) beam–panel; (c) panel–panel.

2.2. Assembly process

The assembly process is expected to be conducted by non-experienced workers in disaster areas. In this context, an assessment of the prototype assembly was carried out to analyse the feasibility of the process. The assembly process is started by placing the four columns in their specified positions (Fig. 5a), and connecting them with three beams (Fig. 5b). The installation of the last beam is postponed to the end of assembly process in order to facilitate the introduction of the floor panels. Hence, the next stage of the assembly process is the installation of the first sandwich panel, by handling and mounting it along the beam–panel connections; as can be seen in Fig. 5c, panel is sliding along the tubular profiles fixed to the beams. Once the first panel is in its final position, and the panel–panel connector is mounted (Fig. 5d), the second panel is installed in a similar way (Fig. 5e). Finally, to complete the assembly process, the final beam is placed in its position (Fig. 5f). All this procedure is performed in less than 2 h by three persons without any special equipment, evidencing that the prefabricated prototype may be suitably assembled by non-experienced workers in a short period of time, and without the need of any special tool and equipment, which are normally scarce in a disaster area.

3. EXPERIMENTAL PROGRAM

The following subsections provide details of the experimental programme in terms of material characterisation, test specimen, setups and procedures. The tests were carried out in the Laboratory of the Structural Division of the Civil Engineering Department of the University of Minho (LEST).

3.1. Material characterization

Both GFRP profiles and sandwich panel GFRP skins were characterised by performing tensile tests according to ASTM D3039 [25]. Several tensile specimens with dimensions of 250 x 25 x 5mm³ were extracted from the profiles, as well as from the sandwich panel skins in the longitudinal and transverse directions. Specimens were mounted in the universal testing machine, with a grip distance of 150 mm, and monotonically loaded with a head displacement rate of 2 mm/min up to failure.

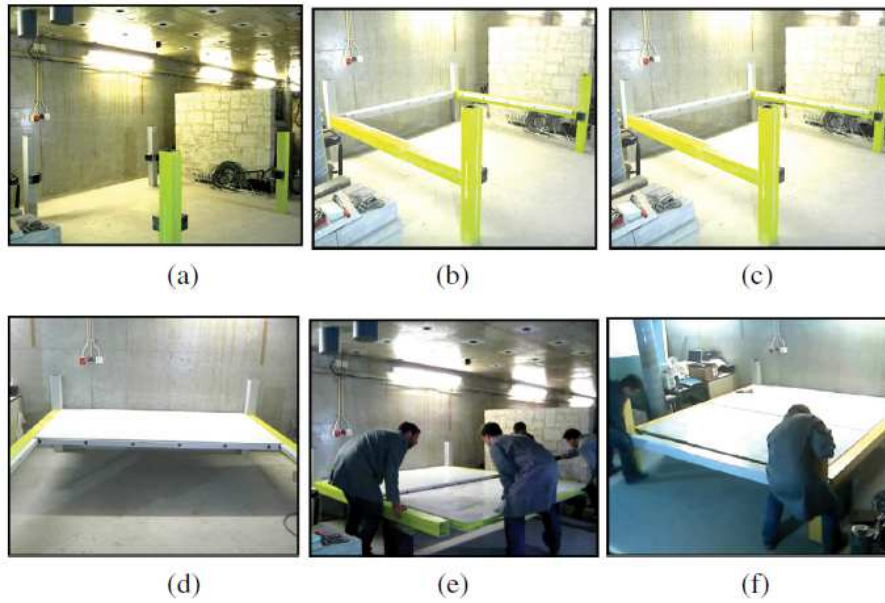


Fig. 5. Assembly process: (a) columns placement; (b) attaching the beams to the columns; (c) first panel mounting; (d) sliding the first panel to its correct position; (e) second panel installation; (f) installation of the final beam.

PU foam core mechanical properties were evaluated under compression and shear. Flatwise compression properties of PU foam were determined according to ASTM C365-03 [26]. Compression tests were performed on prism-shape coupons with the dimensions of $70 \times 70 \times 50 \text{ mm}^3$ under displacement control in a universal testing machine. Shear properties of PU core was determined according to ASTM C273-00 [27] standard. Five coupons with the dimensions of $720 \times 50 \times 60 \text{ mm}^3$ were tested. The tests were performed in a universal testing machine with displacement control at a speed of 0.5 mm/min .

3.2. Static and dynamic studies on the assembled prototype

As previously referred, the lightweight prototype was designed to be the floor element of a residential house, and therefore it was necessary to analyse its performance when submitted to the serviceability vertical loads.

The response of the prototype under flexural loads was assessed by applying a uniform distributed load, representing a characteristic live load of 2 kN/m^2 in accordance with Eurocode 1 [28]. The structure was manually loaded and unloaded employing filler bags (20 kg of each) in two layers, each one of 12 bags, resulting in a uniform distributed load of 1 kN/m^2 per layer. Loading and unloading operations were performed fast to avoid any potential creep effect. Table 1 schematically represents the loading and unloading sequences of the four tests. Fig. 6 illustrates different phases of these tests. Monitoring arrangement is shown in Fig. 7: seven LVDTs (D1–D7) with a stroke ranging from 25 mm to 50 mm were placed at the bottom surface of the slabs's prototype, four in the

beams (D1–D4), and three in the panels (D5–D7), to measure vertical deflections, while eight TML PFL-30-11-3L strain gauges (S1–S8) were bonded to the beams (S7 and S8) and panels (S1–S6) to register the longitudinal and transverse strains during the loading process.



Fig. 6. Distinct phases of the performed tests.

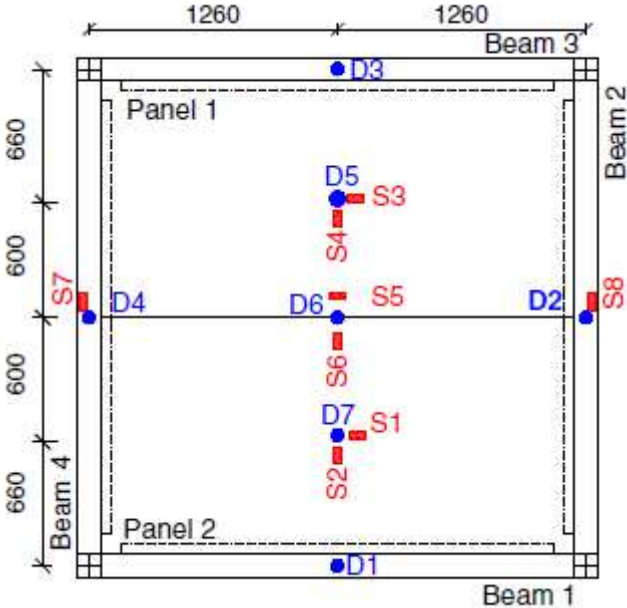


Fig. 7. Instrumentation layout for static tests in the assembled prototype: Positions of LVDTs (D_i , $i = 1-7$) and strain gauges (S_j , $j = 1-8$).

3.3. Full scale flexural test on single sandwich panels

Once the previous tests were performed, sandwich panels were removed from the assemblage, and then they were independently tested under a flexural service load. These tests are illustrated in Fig. 8, and were conducted in accordance with ASTM C393 [30], following two load schemes: (i) four-point bending test, and (ii) three-point bending test.

Table 1. Loading/unloading phases schemes.

Phase	Test 1	Test 2	Test 3	Test 4
Phase 0				
Phase 1				
Phase 2				
Phase 3				
Phase 4				
Phase 5				
Phase 6				
Phase 7				
Phase 8				

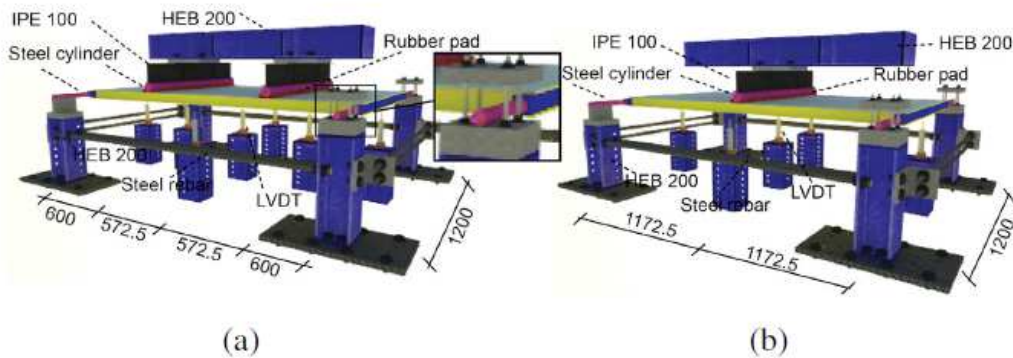


Fig. 8. Schematic representation of the sandwich panel flexural test under service loads: (a) four-point bending test; (b) three-point bending test (all units in millimetres).

The tests were designed in order to introduce a maximum bending moment in the sandwich panel as the previous tests with uniformly distributed load. To apply point loads that introduce a maximum bending moment equivalent to the characteristic live load of 2 kN/m^2 , the panels were subjected to a load of 2.75 kN and 5.5 kN for three-point and four-point bending tests, respectively. Regarding the panel's support conditions, one of the supports allowed

free sliding of the panel, while the other introduced pinned support conditions. A tubular steel profile of 50 x 50 x5mm³ cross section was fixed at each ends of the sandwich panels, and a steel roller with a diameter of 32 mm was placed inside that tubular profile in order to allow free rotation of the panel ends. The monotonic load was applied by a hydraulic jack, and transferred to the panels by means of longitudinal IPE 100 profiles with steel rollers of 20 mm of diameter welded at their bottom flange. A load cell of 300 kN with a precision of 0.05% was used to measure the load, while deflections in the panels were monitored under supports, midspan and in loaded sections by LVDTs with a measuring stroke of 100 mm.

3.4. Small scale tests on sandwich panels

After carrying out the previous tests (full scale flexural test on single sandwich panels), small specimens were extracted from the tested sandwich panels with the purpose of conducting a series of flexural and creep tests. The following subsections provide details of test specimens, setup and procedure.

3.4.1. Small scale flexural tests on sandwich panels

One-way static behaviour of sandwich panels up to failure was investigated according to ASTM C393 standard [29]. Four-point bending tests were carried out with the following two groups of specimens: (i) with an end GFRP ‘U’ profile (P1U and P2U), and (ii) without that profile (P1 and P2). The first group of specimens (P1U and P2U) were tested under a shear span of 300 mm, being the clear span 1150 mm and width of 350 mm (Fig. 9a). The supports were designed in a similar way to the one described in previous section (i.e., by placing a steel roller inside a tubular steel profile). For the second group of specimens (P1 and P2), shear span and panels width were 300 mm and 350 mm respectively, but the clear span was limited to 900 mm. In this case, supports were materialised by steel rollers placed at both ends under the specimens (Fig. 9b).



Fig. 9. Test setup for four-point bending tests up to failure of specimens: (a) with GFRP ‘U’ profile (P1U and P2U); (b) without GFRP ‘U’ profile (P1 and P2) (all units in millimetres).

Loads were applied by a hydraulic jack and were monitored using a load cell of 200 kN with a precision of 0.05%. A steel spreader IPE-beam profile and steel rollers were used to transfer the load to the panels. Additionally, rubber pads were placed between the specimens and the steel rollers to avoid any indentation failure [30–33]. Vertical displacements were recorded by five LVDTs with a stroke ranging from 25 mm to 50 mm, placed on the supports, mid-span and under loaded sections. Moreover, specimens were instrumented in tension and compression skins with TML PFL-30-11-3L strain gauges, placed at the intersection of the midspan section of the specimen with its longitudinal axis.

3.4.2. Small scale creep tests on sandwich panels

Similar to the flexural test, two panels with an end GFRP ‘U’ profile (P3U) and without that profile (P3) were prepared to study creep behaviour of sandwich panels. Specimens were tested in bending for a period of 263 days (6312 h) to assess flexural viscoelastic behaviour as well as long term shear deformation of PU.

Four-point bending tests were carried out with the same test setup configurations described in the previous subsection, except the loading conditions (see Fig. 10). A total load of 1.7 kN was applied. This load corresponds to 24% of its ultimate strength. Vertical displacements were measured by using three mechanical dial gauge displacement indicators, with 0.01 mm of precision. These dial gauges were placed underneath of GFRP bottom skin of the panels, under the loading points and at the mid-span of the panels. These panels were placed in a climate chambering room for the total duration of the test, with controlled temperature and humidity. Average temperature and relative humidity registered were 21 ± 0.5 °C and 60%, respectively.

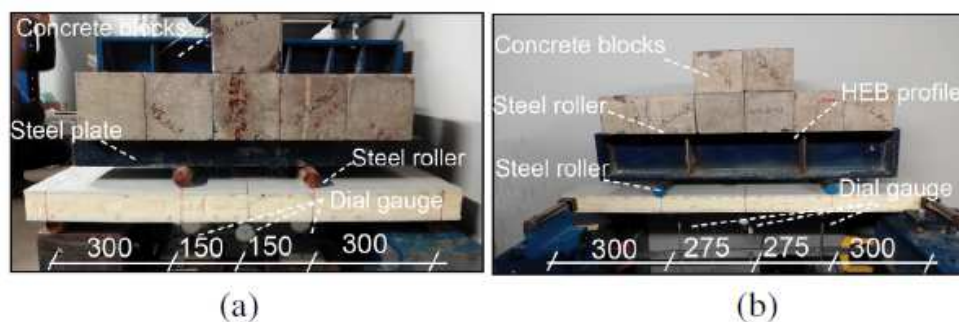


Fig. 10. Test setup for creep test: (a) panel without GFRP ‘U’ profile (P3); (b) panels with GFRP ‘U’ profile (P3U) (all units in millimetres).

4. RESULTS AND ANALYSIS

4.1. Material characterization

The tests carried out on GFRP profiles coupons show a linearelastic behaviour until failure. All of the tested specimens failed in a brittle manner, being the failure located on the middle part of the specimens. From the performed tests an elastic modulus (E) of 28.10 GPa with a coefficient of variation (CoV) of 5.20% was obtained, whereas for the case of the ultimate tensile strength (σ_u) of 327.10 MPa (CoV = 8.60%) was attained.

From the tensile tests conducted on the GFRP skins it was observed that the skin material also presented a linear-elastic behaviour until failure. Similar to what was observed in the GFRP profiles characterisation, all the specimens failed in a brittle manner in their middle height with the failure surface located perpendicularly to the specimen's longitudinal axis. From the performed tests an elastic modulus (E) of 9.60 GPa (CoV = 7.40%) and 10.30 GPa (CoV = 8.01%) were obtained for the longitudinal and transversal directions respectively, whereas for the case of the ultimate tensile strength (σ_u), values of 117.00 MPa (CoV = 10.40%) and 116.90 MPa (CoV = 24.70%) were attained for the longitudinal and transversal directions respectively.

The compression tests showed the typical nonlinearity of the PU foam core with three distinct parts: the linear elastic branch that is followed by a plastic plateau with nearly constant stress, and continues with a strain-hardening branch at large deformation stage [34], which corresponds to the progressive densification of the material [35]. From the performed tests an elastic modulus (E) of 9.10 MPa (CoV = 9.01%) was obtained, whereas for the case of the ultimate compressive strength (σ_u), a value of 0.30 MPa (CoV = 10.02%) was attained. It must be mentioned that values for compression corresponded to the first branch (linear elastic part).

Regarding the shear tests, PU foam core coupons show linear elastic behaviour until failure, which was brittle with the formation of failure surfaces at an angle of nearly 45°. From the performed tests a shear modulus (G) of 3.15 MPa (CoV = 12.07%) was obtained, whereas for the case of the ultimate shear strength (σ_u) a value of 0.15 MPa (CoV = 10.02%) was attained.

4.2. Static tests on the assembled prototype

The measured deflection–time and strain–time relationships in each carried out test are plotted in Fig. 11. The end of each loading/unloading operation is recognisable by the sudden change observed in the curves. In fact, the presence of small deflections and strains at the end of each of the loading/unloading phases is the consequence of having three persons on the top of the panels during the loading/unloading procedures. Furthermore, it is interesting to mention that once all the load was applied, the four performed tests gave the same results in terms of deflections

and strains; thus, all tests can be considered as equivalent, and differences between each one are mainly due to the loading/unloading scheme.

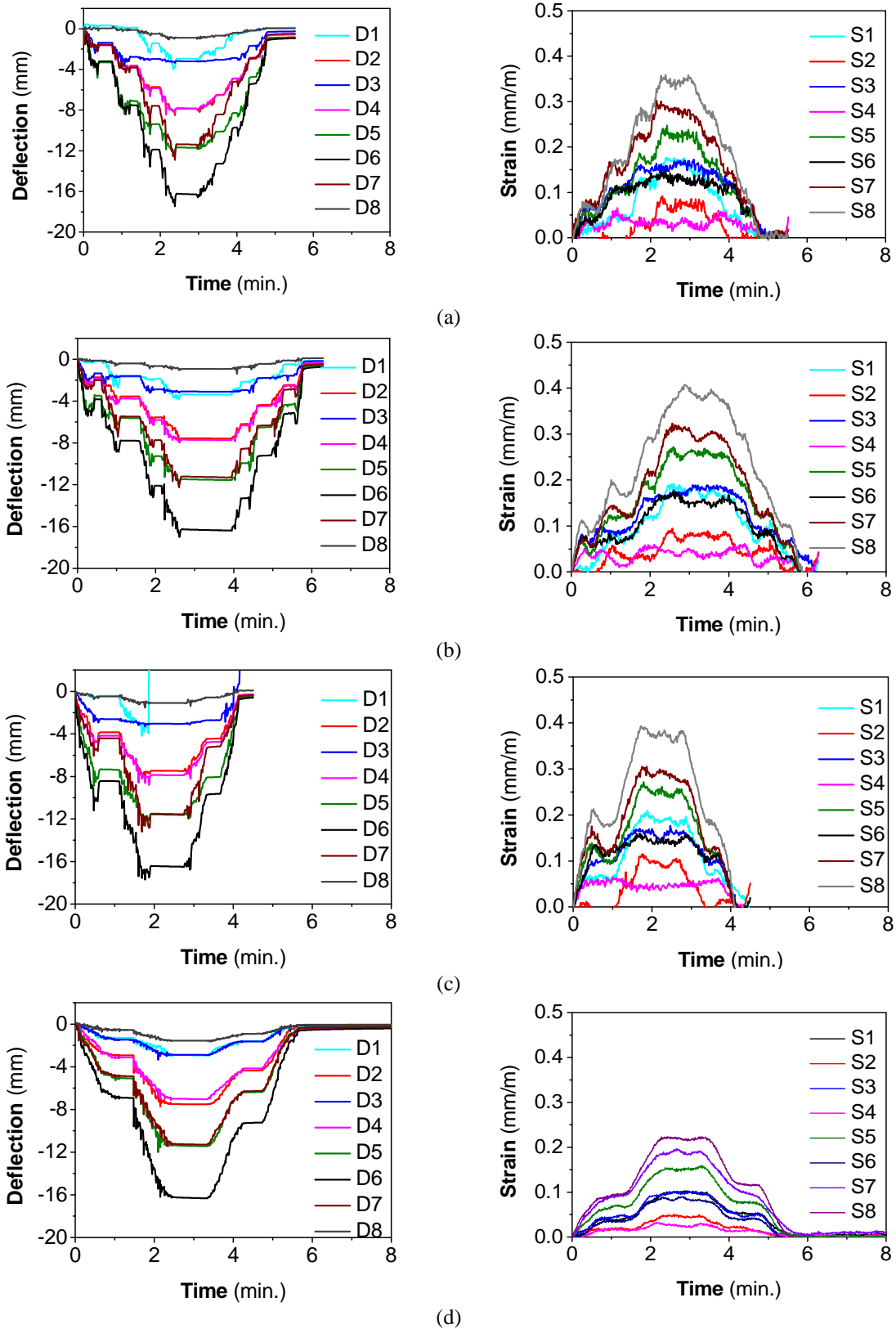


Fig. 11. Static test results on the assembled prototype: (a) Test 1; (b) Test 2; (c) Test 3; (d) Test 4.

Based on the obtained deflections at the end of loading process, four groups of LVDTs could be identified (see Table 2). The first group includes the LVDT placed at the middle of the two panels joint (D6 – see Fig. 6), which recorded a maximum value of about 16 mm. The second group are those LVDTs placed at the centre of the two panels (D5 and D7), which measured a value of around 12 mm. The third group corresponds to the LVDTs placed on longitudinal beams (D2 and D4), i.e., those beams placed perpendicularly to the panel–panel connection (beams 2 and 4), in which a deflection of approximately 7.5 mm was registered. Finally, the fourth group of LVDTs (D1 and D3) is related to those placed on transverse beams (beams 1 and 3), which recorded a value of 3 mm.

Table 2. Maximum deflections (in mm) registered in the assembled prototype subjected to a uniform load of 2 kN/m².

Test	Panels joint (D6)	Middle of panels (D5 and D7)	Longitudinal beams (D1 and D3)	Transverse beams (D2 and D4)
Test 1	-16.49	-11.93	-3.46	-7.91
Test 2	-16.29	-11.48	-3.09	-7.56
Test 3	-16.41	-11.56	-3.03	-7.47
Test 4	-16.21	-11.44	-2.87	-7.49

Similarly, the strain gauges may also be grouped in five groups. The first group involves the strain gauges bonded at the centre of the joint between the two panels in the longitudinal direction (S5), which measured a strain value of around 0.25 mm/m. The second group corresponds to those gauges placed in the longitudinal direction in the middle of the panels (S1 and S3), which recorded a value of nearly 0.17 mm/m. The third group comprises the strain gauge located at the centre of the joint between the two panels in the transverse direction (S6), which registered a value of 0.15 mm/m. The fourth group consists of those gauges measuring transverse strains in the middle of the panels (S2 and S4), where a strain value of about 0.05 mm/m was recorded. Finally, the fifth group is comprised by those strain gauges placed in the middle of the two beams 4 and 2 (S7 and S8), where a maximum strain of 0.35 mm/m was registered. Table 3 lists the maximum values of strains registered in the prototype.

Table 3. Maximum strains (in mm/m) registered in the assembled prototype subjected to a uniform load of 2 kN/m².

Test	Group one (S5)	Group two (S1,S3)	Group three (S6)	Group four (S2,S4)	Group fifth (S7,S8)
Test 1	0.23	0.13	0.13	0.05	0.35
Test 2	0.26	0.17	0.16	0.05	0.37
Test 3	0.26	0.14	0.14	0.05	0.38
Test 4	0.15	0.09	0.08	0.04	0.22

From the analysis of the displacements and the strains some information can be extracted. Analysing the strains recorded in the first and second groups of gauges (S5 and S1, S3), and in the third and fourth groups (S6 and S2, S4) it is verified that the level of strains registered in the centre of each panel is significantly different from the

level of strain recorded in the centre of the joint between the two panels. This indicates that the panels did not present one-way bending behaviour. Likewise, when compared the first and second groups of LVDTs (D6 against D5 and D7) it is revealed that floor panels presented a two-way bending behaviour, being the bending moments in longitudinal direction (i.e., where beams 2 and 4 work as support) higher than in the transverse direction. The response of the panels implies that beam–panel connection was tight, assuring a high degree of connectivity of the panel to the supports. Regarding to the third and fourth group of LVDTs, their measurements show that beams 2 and 4 presented almost double deflection of beams 1 and 3, demonstrating the different load level transferred by the panels to these supporting beams. Furthermore, the largest strains were recorded in beams 2 and 4 (last group of gauges, S7 and S8). Finally, it should be referred, as expected, for the load levels applied the system behaved linearly, since after removing the loads negligible displacements and strains were registered.

4.3. Full scale flexural test on single sandwich panels

Load versus midspan deflection for sandwich panels in service limit state under three point and four-point bending tests are plotted in Fig. 12. Both tests presented a very similar response, which is an indicator of the elastic behaviour of the composite sandwich panels under characteristic live loads. The flexural stiffness (K), defined as the ratio between the maximum applied load and its corresponding midspan deflection (δ_{max}), was quite similar in both testing configurations (Table 4), confirming the same flexural behaviour of both floor panels under serviceability loads.

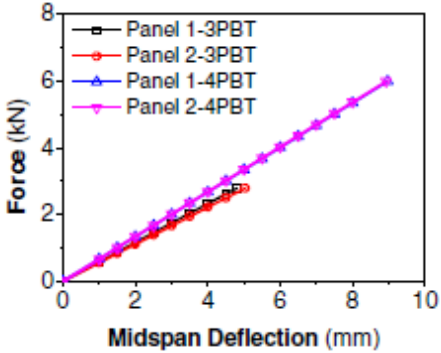


Fig. 12. Load–midspan deflection of sandwich panels under service loads.

Table 4. Three-point and four-point bending tests results for sandwich panels under service loads.

Panel	Three-point bending test		Four-point bending test	
	δ_{max} (mm)	K (kN/mm)	δ_{max} (mm)	K (kN/mm)
Panel 1	4.80	583	8.96	669
Panel 2	5.03	556	8.92	672

4.4. Small scale tests on sandwich panels

4.4.1. Small scale flexural tests on sandwich panels

The load–deflection curves for the two types of small sandwich panel specimens tested, i.e., panel specimens with (P1U and P2U) and without GFRP ‘U’ profile in the supporting extremities (P1 and P2), are presented in Fig. 13. For the case of specimens without GFRP ‘U’ profile in their supporting extremities, results show that the relation between load and midspan deflection was fairly linear up to failure. Load capacity of these specimens increased linearly and continuously until reaching a load of 7 kN, at a deflection of 14 mm; at this moment, specimens failed abruptly due to shear rupture of the core. Conversely, as Fig. 13 shows, for the case of sandwich panels with end GFRP ‘U’ profile, the relation between load and displacement was linear until a load of about 4 kN (which is nearly 60% of the maximum load). Once reached that load, a small reduction in the stiffness was observed due to delamination of the bottom GFRP skin in the maximum flexural zone. However the specimens were capable of supporting higher load, registering a slightly drop at a load of 5 kN also due to delamination of the bottom skin. Above this load stage, the stiffness of these panels has gradually decreasing up to the sudden brittle failure that occurred at a load of about 7 kN, caused by the rupture of the core material in the vicinity of the support.

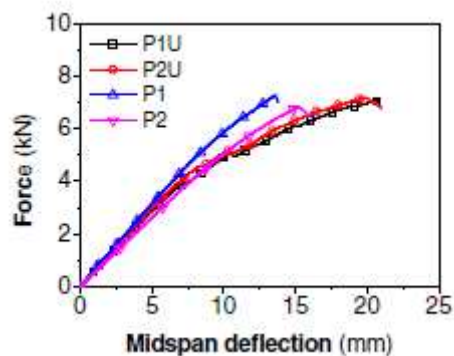


Fig. 13. Load–midspan deflection curves: (a) specimens without end GFRP ‘U’ profiles; (b) specimens with end GFRP ‘U’ profiles.

Obtained results show that nearly the same ultimate load was registered in both types of specimens. Fig. 14 shows the moment–curvature diagram at the midspan cross-section for four-point bending tests load configuration, where the curvature was calculated using the information given by the strain gauges placed at the midspan cross-section (top and bottom skins). Both types of specimens present a linear behaviour response before failure, being their flexural stiffness (defined as the slope of the moment–curvature diagram) very similar in all the tested specimens. This confirms that introducing the end GFRP profile in the panels did not have any significant effect in terms of flexural stiffness. Table 5 include the values for the ultimate moment (M_u), the ultimate load (P_u), the maximum

deflection (δ_u), the initial stiffness (K) defined as the slope of the force and deflection in the linear part, the maximum longitudinal strain on the top and bottom skins (ϵ_{ut} and ϵ_{ub} , respectively), the maximum flexural stress (σ_u), and the maximum average shear stress in the core (τ_u) obtained according to Eqs. (1) and (2), based on equilibrium analysis [36].

$$\sigma = \frac{M}{b \cdot d \cdot h_f} \quad (1)$$

$$\tau = \frac{\partial M}{\partial x} \frac{1}{b \cdot d} \quad (2)$$

where d is the distance between the centroids of the skins, $d = h_c + h_f$, where h_c and h_f are the core and skin thicknesses, respectively, and b is the width of the panel.

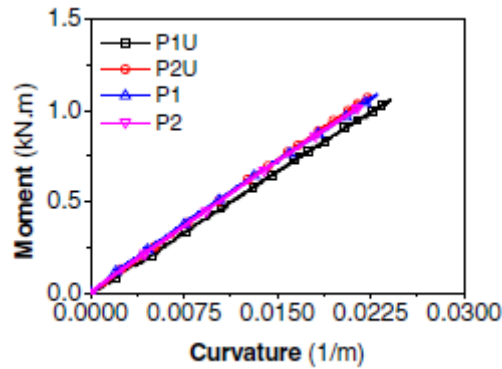


Fig. 14. Moment–curvature diagrams: (a) specimens without end GFRP ‘U’ profiles; (b) specimens with end GFRP ‘U’ profiles.

Failure modes are presented in Fig. 15. Shear failure of the core was the mechanism governing the behaviour of the specimens tested without end ‘U’ profiles (P1 and P2). This failure could be explained by the fact that the registered foam core shear stress in the specimens (see Table 5) exceeded maximum shear stress obtained in material characterisation. Shear failure occurred in the shear span, with a crack angle of 45°. The propagation of these shear cracks followed toward the skins causing core-skin debonding. In the case of specimens with end GFRP ‘U’ profile (P1U and P2U), the failure was governed by the debonding between the bottom face of the GFRP ‘U’ profile and the GFRP bottom skin, followed by an abrupt formation of a tensile fracture surface on the core materials due to its residual tensile strength, and propagation of the failure surface at the core-top GFRP skin. Hence, the detachment process between GFRP ‘U’ and GFRP bottom skin is eminently a nonlinear phenomenon, which justify the nonlinear response of these panels.

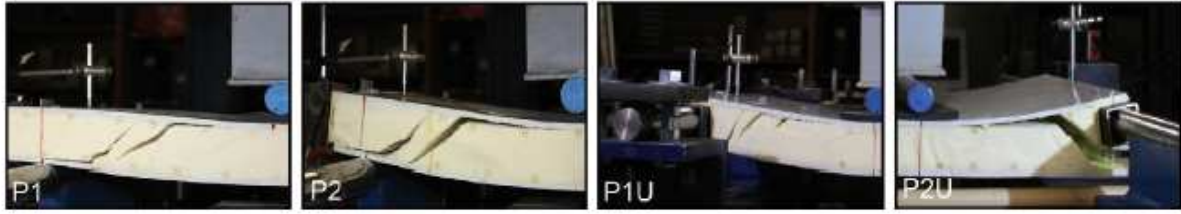


Fig. 15. Failure modes.

Table 5. Summary main results from the tests up to the failure.

Specimen	M_u (kN·m)	P_u (kN)	δ_u (mm)	ϵ_u (μ strain)		σ_u (MPa)	K (kN/mm)	τ_u (kPa)
				ϵ_{ut}	ϵ_{ub}			
P1	1.09	7.27	13.59	-807	804	9.58	47.45	159.80
P2	1.02	6.83	15.20	-590	941	9.00	47.14	150.11
P1U	1.06	7.06	20.67	-838	854	9.31	43.91	155.16
P2U	1.07	7.18	20.01	-714	859	9.47	47.93	157.80

Bending strain–stress relation at top and lower skins for the specimens tested is depicted in Fig. 16. The strain values were those registered in the strain gauges applied on the top and bottom surfaces of the panels, while the stresses were calculated based on the equilibrium of tension and compression forces on the skins, according to Eq. (1) [36]. A quite linear behaviour for strain–stress in both specimens before any failure can be observed, being a consequence of the linear strains measured in the GFRP skins, which at the same time is a reflection of the linear behaviour exhibited by this material. Moreover, when calculating the elastic modulus, the average elasticity modulus obtained in the GFRP material characterisation (around 9.5 GPa) is reached. It is interesting to mention that all the specimens failed at a stress and a strain of approximately 9 MPa and 850 mm/m, respectively. These levels of stress and strain are only 7% of the ultimate stress and strain of the GFRP material obtained from the direct tensile tests.

4.4.2. Small scale creep tests on sandwich panels

Load versus mid-span deflection relationship for the panels P3 and P3U are illustrated in the Fig. 17a and b, respectively. The applied 1.7 kN induced an immediate elastic deformation of 3.33 mm and 3.5 mm for panels P3 and P3U, respectively. Keeping that load constant during almost nine months, the mid-span deflection in both P3 and P3U increased to around a 116% of the elastic deflection. This evidences the importance of considering long term deformation in composite sandwich panels. Moreover, it was observed that support condition did not have any major effects in long term behaviour of the panels.

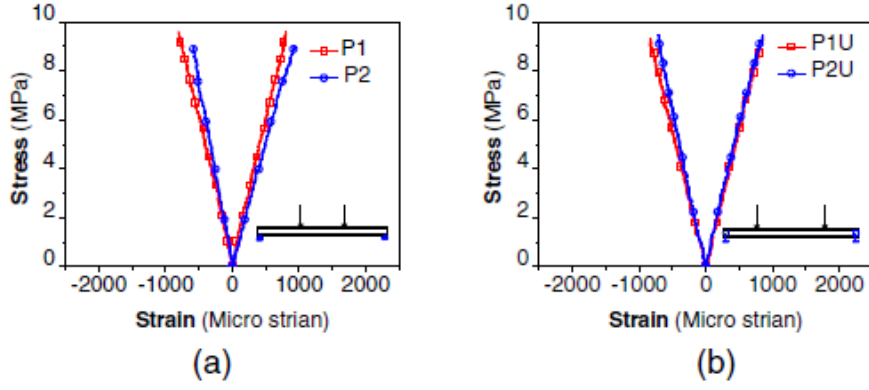


Fig. 16. Stress–strain curves: (a) specimens without end GFRP ‘U’ profiles; (b) specimens with end GFRP ‘U’ profiles.

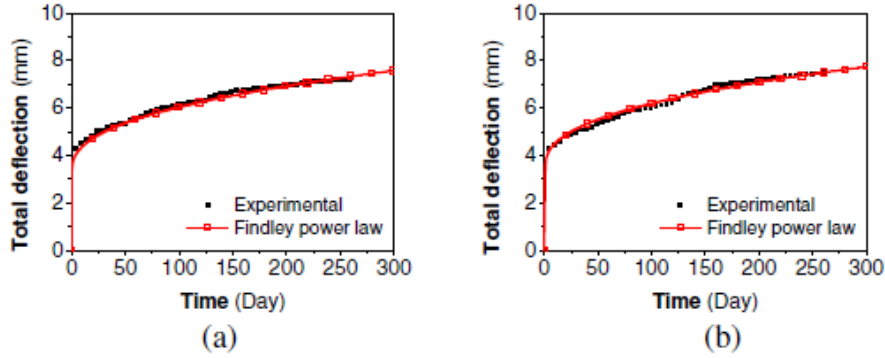


Fig. 17. Time–midspan deflection: (a) P3; (b) P3U.

Findley power law was used to estimate viscoelastic deformation of the panel by the time, following Eq. (3):

$$\delta = \delta_0 + m \times t^n \quad (3)$$

where δ is the time dependent deflection (in mm), δ_0 is the instantaneous deflection (in mm), m is the creep amplitude, t is the time after application of load (in days), and n is the time exponent. Power law has fitted the experimental results by using a creep amplitude of $m = 0.41$ and a time exponent of $n = 0.41$ in both types of the panels. These parameters were obtained with a coefficient of determination (R^2) of 99%. By using Eq. (3) with these values for its parameters, and considering a service life of 5 years for the type of emergency applications that the prototype is designed for, a viscoelastic deformation 252% higher than the initial elastic deflection is estimated at the end of this period.

According to CNR guideline [37], the maximum long-term deflection in a composite structure should be less than $L/250$, being L the flexural span. An estimation of the maximum slab deflection registered in the floor prototype may be obtained if the deflection experimentally registered (see Table 2) in the longitudinal beams (beams 2 and

4) is subtracted from the maximum deflection registered in panels. Hence, deflection in long-term for the prototype studied (δ_{LT}) can be obtained as:

$$\delta_{LT} = \beta \cdot \delta_{qp} \quad (4)$$

where β corresponds to the estimated coefficient due to effects of creep (equal to 2.52 as indicated above); and δ_{qp} represents the experimental measured deflection in the mid-span of the floor panels for a load corresponding to the quasi-permanent load, i.e., the dead load and the part of the live load (usually a 30%). From Eq. (4), a value of 6.65 mm is estimated as long-term deflection for the prototype. Taking into account that the length of panels is equal to 2400 mm, hence ratio 2400/250 is equal to 9.6 mm; consequently, it can be observed that the proposed designing for the modular system satisfies the CNR [37] recommended criterion.

5. NUMERICAL SIMULATION

5.1. General approach

The proposed modular prototype was numerically simulated by a nonlinear three-dimensional finite element (FE) analysis. Calibration of the model was performed based on the experimental results. The simulation enabled to assess the stress distributions in prototype components, such as beams and panels, as well as evaluate the global behaviour and load transfer mechanism of the connections, and assess their influence in load distribution.

5.2. Numerical model description

The prototype was modelled by a 3-D finite element analysis with the same geometry of the experimentally tested elements. All prototype constituents, i.e., GFRP skins, PU foam core, GFRP beams and columns, were modelled using 3D hexahedral deformable solid elements with 8 nodes and 3 degrees of freedom per node. After some preliminary analysis have been conducted, an approximately size of the elements equal to 10 mm edge was found to be optimal in terms of both accuracy convergence and computational time of the simulation. The overall FE model for the tested modular floor building submitted to uniform static load is shown in Fig. 18. Loading and boundary conditions were applied in accordance with the particularities of the experimental test setup. In three of the columns the displacement in the z direction of the nodes located in the surface in contact to the supporting pavement is prescribed, while in the other column all the displacement degrees of these nodes were prescribed. A uniform load of 2 kN/m² was applied on the top surface of the sandwich floor panels. Proper loading arrangement and boundary condition depicting the experimental setup is shown in Fig. 18. Nonlinear static analysis enabling geometric nonlinearity based on direct method 'Full Newton Solution Technique' was performed.

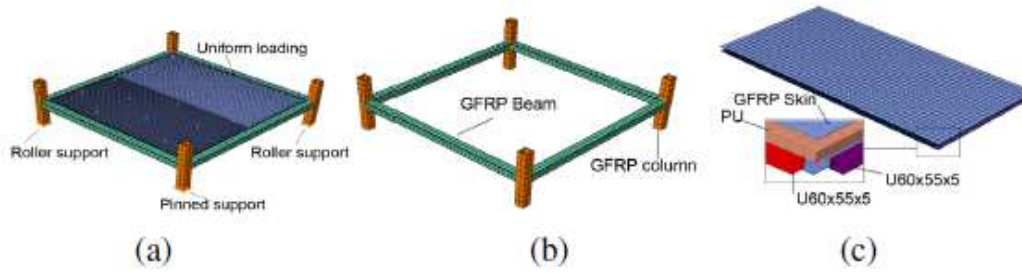


Fig. 18. FE model perspective of the tested panel: (a) overall view; (b) GFRP frame structure; (c) sandwich floor panels with constituent material.

Constitutive relation toward material behaviour of sandwich panel components were adopted according to the performed material characterisation tests. The GFRP skins have a quasi-isotropic lay-up, so isotropic linear elastic material with an elastic modulus of 9.60 GPa, Poisson's ratio of 0.3 and ultimate stress of 117 MPa were used to represent the GFRP skin mechanical behaviour. In the case of PU foam core material, an elastic-plastic constitutive behaviour was assumed, with an elastic modulus of 6 MPa, a Poisson's ratio of 0.15 and plastic pseudo-yield stress of 0.36 MPa. The GFRP pultruded profiles were modelled assuming linearelastic orthotropic material properties with an elastic modulus of 28 GPa and ultimate tensile stress of 415 MPa in the parallel to the fibre direction (longitudinal direction), and elastic modulus of 13 GPa and ultimate tensile stress of 180 MPa in the perpendicular to the fibre direction (transversal). Interactions between the sandwich panel's components were assumed as a tie constrain representing full composite action. Contact connections between profiles and U-shaped GFRP profiles of sandwich panels were modelled by a surface interaction: in the normal direction a "hard" contact is assumed, meaning that no penetration is allowed between the two surfaces, with no limit to the magnitude of contact pressure that can be transmitted when the surfaces are in contact. Behaviour in the tangential direction was modelled with Coulomb friction model, with a friction coefficient equal to 0.2 and with no adhesion.

5.3. FE model results

A comparison between the experimentally measured deflections and predicted ones by the FE simulation at different positions is provided in Table 6. Furthermore, experimentally obtained tensile strain are also compared with the predicted ones by the FE simulation. In general, a good agreement is observed between the FE model and the experimental prototype. This validates the developed model and enables its use for predicting the flexural behaviour of the proposed modular floor prototype.

The colour representation of the vertical displacement field (in y direction) obtained from the FE model is depicted in Fig. 19. A maximum vertical deflection of 15.89 mm was registered in the central part of the pavement, in the join of the two sandwich panels. It is interesting to note that, the GFRP connector bridging internally the two

panels while was not connected to the transversal beams. As a results, the contour plot resemble to the typical one as a continuous slab. However a predominant working direction in the longitudinal direction can be observed. Moreover, this is confirmed by the deflection of the beams where one can notice that deflection in the frame beams placed orthogonal to the panels' length reach a slightly higher deflection than beams parallel to them.

Table 6. Comparison between experimental and numerical FEM results.

	Experimental	FEM
<i>Deflection (mm)</i>		
Panels joint (D6)	16.2	15.9
Middle of the panels (D5 and D7)	11.4	11.0
Longitudinal beams (D1 and D3)	2.9	2.8
Transverse beams (D2 and D4)	7.5	6.5
<i>Strain (mm/m)</i>		
Group one (S5)	0.25	0.33
Group two (S1 and S3)	0.17	0.18
Group three (S6)	0.15	0.12
Group four (S2 and S4)	0.05	0.06
Group five (S7 and S8)	0.35	0.48

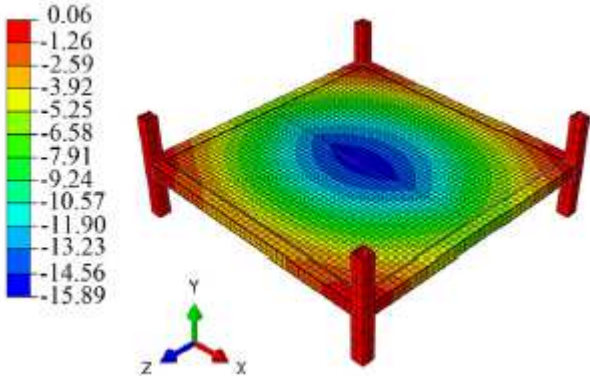


Fig. 19. Deformed shape for the FE mode (deflections, in m).

Stresses developed at the external face of bottom GFRP skins in the floor sandwich panels, due to the load applied (2 kN/m^2) in the longitudinal and transversal directions, are shown in Fig. 20. Checking the level of stresses revealed that all the stresses were below the ultimate strength limit with adequate safety factor. A direct conclusion from this observation is that the proposed panels withstand the ULS load level as they are only 50% above the SLS limit according to Eurocode 1 [28]. The difference of stress distribution at the middle of the panels and through their edges evidence that panels are working as a two-way slabs, being the longitudinal direction the main working direction. Connection between sandwich panels and GFRP beams elements remains a challenging issue. From Fig. 20 it can be observed that the presence of the connections provide some restriction along the support, thus contributing to reduce the overall floor sandwich panels flexibility. However, the amount of this restriction in

reducing sandwich panel's deflection is not clear. It can be seen that the type of connection used does not act as a fully fixed support and thus, it would resemble to a semi-fixed connection. Hence, proposed connection can be considered as a spring with a characteristics stiffness k_{sc} . Therefore the total deflection at panels midspan joint (δ) would be the sum of the deflection due to the fixed support (δ_c) and the connection flexibility (δ_0), i.e., $\delta = \delta_c + \delta_0$.

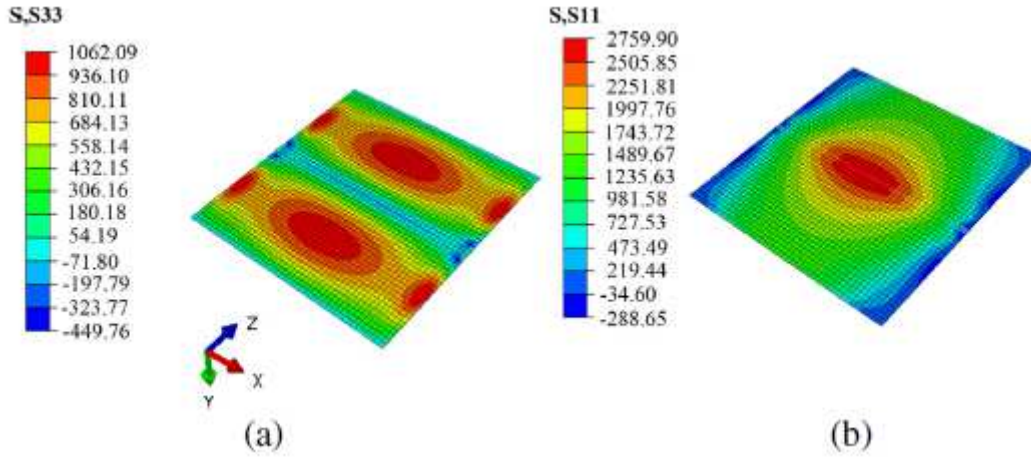


Fig. 20. Stress in the bottom surface of lower GFRP skin: (a) longitudinal direction; (b) transversal direction (stresses, in kPa).

To overcome that issue, a new simulation was carried out by considering fixed support condition between the floor panels and the GFRP beam elements. Fully composite action was assumed by using a tie interface between GFRP square profiles and GFRP ‘U’ profiles. Fig. 21 shows the numerical load–midspan deflection obtained by considering fixed-support conditions compared with the deflection obtained by considering the real connections. Hence, the difference between the two curves corresponds to the deflection caused by the connection flexibility (equal to 5.39 mm). Based on that figure, the proportion on stiffness, defined as the slope between load and deflection, may be expressed by Eq. (5):

$$\frac{k_c}{k_{sc}} = \frac{\delta_c + \delta_0}{\delta_c} \quad (5)$$

where k_c is the stiffness of panel in fixed support conditions and k_{sc} is the stiffness of panels in semi-fixed support conditions.

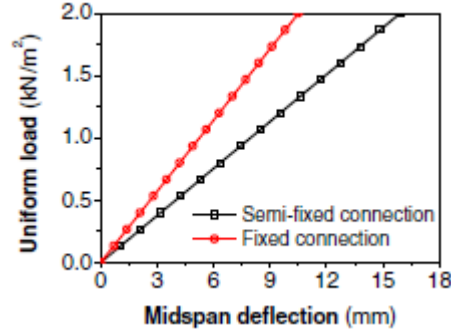


Fig. 21. Load–midspan deflection in fixed and semi-fixed connection.

Eq. (5) could be modified in other term as Eq. (6), where Π is the stiffness reduction factor.

$$\frac{k_{sc} + \Pi \cdot k_{sc}}{k_{sc}} = \frac{\delta_c + \delta_\theta}{\delta_c} \quad (6)$$

Once computed, coefficient Π was calculated to be 0.51. Thus, a direct conclusion drawn from here is that, when using the proposed connection in the prototype, which acts as a semi-fixed support conditions, a stiffness reduction of a 51% respect to a fixed support condition can be expected.

5.4. Parametric study

The proposed FE model was shown to be an effective tool for investigating the flexural response of the residential floor modular system. A parametric study was then carried out to explore the potentiality of the proposed material and structural concept for pavements of higher span length in order to have more housing space and, consequently, to extend this concept for other markets.

The parametric study was addressed by changing the thickness of PU foam core (h_c) and span length of the sandwich floor panel (L), while keeping the thickness of the GFRP skin (h_f) and the width of the sandwich floor panel (w) equal to 5 mm and 1200 mm, respectively. Both parameters have significant impact on the stiffness and the deformability of the sandwich floor panel. By changing h_c maintaining h_f constant has the purpose of exploring the variation of panel's stiffness with the minimum cost, since foam is the less expensive constituent of this construction system. By varying L while w is keeping constant has a significant impact on the deformational response of the panel, due to its almost one way slab behavioural character. Maintaining w constant contribute for do not change significantly the transport conditions of these components, since by increasing both L and w above a certain limit the transport costs of these panels will increase. Additionally, the connection conditions between GFRP beams' elements and sandwich floor panels were evaluated for the following two scenarios: (i) semi-fixed

(i.e., like the actual one on the experimentally tested prototype) with the designation of ‘SC’; (ii) fixed connection with the nomination of ‘FC’.

A total of 54 models were created and analysed under serviceability load conditions in residential houses by assuming a uniform distributed load of 2 kN/m² on the top surface of the sandwich floor panels. For deriving relevant conclusions the representative results indicated in Table 7 were selected.

Table 7. Maximum predicted deflection in residential floor modular system components subjected to serviceability load conditions.

h_c/h_f	L (mm)	Maximum deflection (mm)							
		Panels joint		Middle of panels		Longitudinal beams		Transversal beams	
		SC	FC	SC	FC	SC	FC	SC	FC
12	1800	9.5	6.4	6.6	5.5	1.1	1.1	5.5	3.9
	3000	27.8	17.9	19.9	15.7	8.3	7.9	8.9	5.4
	3600	44.5	28.7	33.5	26.1	17.4	16.1	10.7	6.1
	4200	68.2	44.9	54	42.1	32.3	29.2	12.4	6.9
		7.5	5	5.6	4.4	1	0.9	4.8	3.4
16	1800	21.1	13.7	15.5	12.1	7.2	6.8	8.5	4.7
	3000	33.4	21.8	25.7	20.3	13.8	13.2	10.2	5.3
	3600	51.1	35	41.4	33.2	25.5	23.9	11.8	6
	4200	6.8	4	4.8	3.6	0.8	0.7	4.8	2.8
		17	10.3	12.5	9.5	5.3	5.2	7.8	3.9
20	1800	26.2	16.9	21.5	16.2	12.1	11	8.2	4.6
	3000	40.2	26.6	32.5	25.7	20.3	18.9	8	4.9
	3600	9.5	6.4	6.6	5.5	1.1	1.1	5.5	3.9
	4200	27.8	17.9	19.9	15.7	8.3	7.9	8.9	5.4

Table 7 shows that by increasing the panel’s span length the maximum deflection increases in the longitudinal beams due to the more pronounced one way slab character of the panel. This increase rate is reduced by the increase of the ratio $h_c=h_f$ due to the larger contribution of the flexural stiffness of the panel. This observations can be seen in Fig. 22.

By increasing $h_c=h_f$ from 12 to 20 in the shorted panels (L = 1800 mm) has provided a decrease in the maximum deflection that varied between 14% and 37% when the four considered components of the panel and the two connection conditions are analysed, having the highest decrease occurred in the panels with ‘FC’ connection conditions. However, the range of values of the aforementioned decrease in the maximum deflection has decreased with the increase of the panel’s length, having varied between 29% and 41% in the longer panels (L = 4200 mm), In these longer panels, the higher decrease of the maximum deflection occurred in the panels joint, regardless the connection conditions (about 41%).

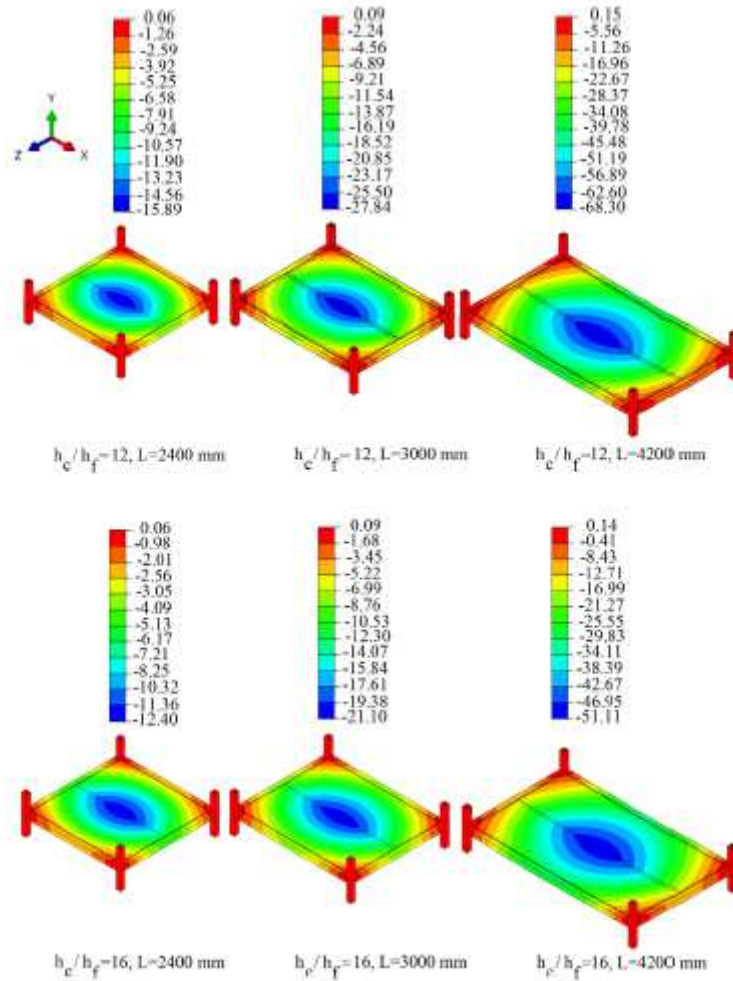


Fig. 22. Vertical deflection of the residential floor modular system under different h_c/h_f ratios and span lengths with 'SC' support condition (in mm).

The maximum deflection for quasi-permanent load conditions (i.e., 30% of the total live load) was computed for the mid-span of the floor modular system (δ_{qp}) in each analysis. The obtained deflections were subsequently manipulated by employing Eq. (4) to capture the long-term performance of the floor modular pavements (δ_{LT}). The results are showed in Fig. 23. It should be noticed that in this figure, the curves are named based on two characters. The first character is the $h_c=h_f$ ratio, while the second character indicates the type of connection between GFRP beams' elements and sandwich floor panels.

Graphics like the one represented in Fig. 23 can be developed for assisting on the design of composite sandwich panels for residential building product applications. By taking the graphic of Fig. 23 as an example of this pre-design approach, and assuming a span length of 3000 mm for the composite floor panel (represented by a vertical dot line), and considering the maximum deflection criterion recommended by CNR [37] (plotted by a horizontal dot line), the panel '20-SC', and all the panels with 'FC' connection conditions are possible solutions, being the

economic criterion critical for the final decision. For the other sandwich panels, do not fulfilling the requirement of maximum deflection, this can be overcome by increasing their flexural stiffness through adopting more internal GFRP ribs.

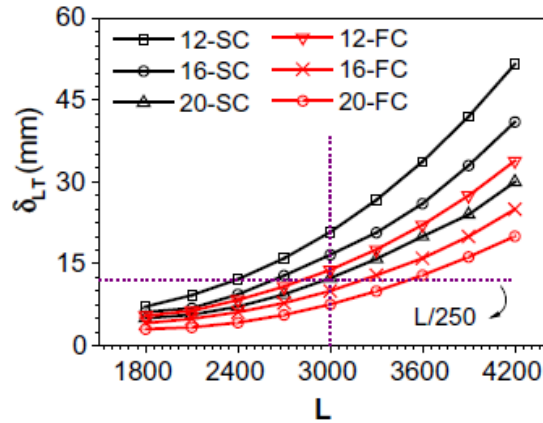


Fig. 23. Flexural response of the residential floor modular system at different conditions.

6. CONCLUSIONS

This paper has presented a series of experimental tests conducted on a composite floor prototype module to be used as a part of a temporary house. The proposed floor prototype consists of four pultruded GFRP beams and two composite sandwich panels (composed of GFRP skins and PU foam core) stabilised by four short pultruded GFRP columns. The work presented here is part of the ClickHouse project, which is aimed to develop a prefabricated housing employing light weight advanced composite materials for being used as an emergency house or temporary dwelling. The experimental programme has evaluated the feasibility of the assembly process, the flexural response of the prototype under residential service loads. Additionally, sandwich panels were independently tested to determine their overall flexural behaviour up to failure. The main concluding remarks drawn from this work can be listed:

1. The GFRP composite sandwich panels and pultruded profiles were integrated in a floor modular prototype. This made it possible to prefabricate a building that is easily transported to the site and rapidly installed.
2. Using the proposed connections and thanks to the lightness of structure members, the assembly/disassembly process of the prototype was performed in less than 2 h by three persons without any special equipment. As such, this functionality illustrates the high potentiality of this system to be used as a prefabricated emergency house.
3. In the assembled structure, even though flexural work was more predominant in one direction, beam–panel and panel–panel connectors forced the floor panels to behave as a two-ways-panning slab.

4. Long-term behaviour of proposed composite sandwich panels were studied with two support conditions: (i) with end GFRP ‘U’ profile, (ii) without that profile. Support conditions were found not have any influence for the creep behaviour of the panels since both panels presented the same viscoelastic behaviour. Findley power law was fitted and predicted maximum deformation of the panels after five years which was 2.5 times higher than initial elastic deformation.

5. In failure tests, fairly linear behaviour was observed for all specimens tested. In specimens with GFRP end ‘U’ profile, small reductions in the stiffness was noticed due to debonding of the lower GFRP skin. However, it was identified that presence of this GFRP profile did not have any significant effect in the flexural strength and stiffness.

6. Shear failure of the core was the mechanism governing the behaviour of the specimens tested without end ‘U’ profiles. On the other hand, in the case of panels with end GFRP ‘U’ profile, panels failed due to the debonding between the bottom face of the GFRP profile and the GFRP bottom skin, followed by an abrupt formation of a tensile fracture surface on the core materials due to its residual tensile strength.

7. A FE model was developed. The model showed to be capable of predicting the actual behaviour of the modular system under designed load. Accordingly, the model was used to assess the behaviour of proposed connection between sandwich panels and GFRP beam elements. It was noticed that employing proposed connection leads to having some degree of freedom in the support and acting this support as a semi-fixed. A stiffness reduction factor of a 52% was computed, meaning that a reduction of around this value occurs in the stiffness of system respect to a fully fixed support condition, resulting in an increment in the floor panel flexibility.

8. A parametric study was carried out to extend the proposed system to other pavements of higher span length in order to have more housing space and, consequently, to spread-out this concept for other markets. From this study design strategies were proposed to support the design of the composite sandwich panels.

ACKNOWLEDGEMENTS

This work is part of the research project *ClickHouse - Development of a prefabricated emergency house prototype made of composites materials*, involving the company ALTO – Perfis Pultrudidos, Lda., CERis/Instituto Superior Técnico and ISISE/University of Minho, supported by FEDER funds through the Operational Program for Competitiveness Factors – COMPETE and the Portuguese National Agency of Innovation (ADI) - project no. 38967. Special thanks are given to company ALTO - Perfis Pultrudidos, Lda., who manufactured all the elements (GFRP profiles and sandwich panels) involved in this work. The authors also want to express their

gratitude to Engineers Mário Alvim and Tomé Santos, for their invaluable collaboration, help and support in this research.

REFERENCES

- [1] Johnson C. Impacts of prefabricated temporary housing after disasters: 1999 earthquakes in Turkey. *Habitat Int* 2007;31:36–52.
- [2] Arslan H, Cosgun N. Reuse and recycle potentials of the temporary houses after occupancy: example of Duzce, Turkey. *Build Environ* 2008;43:702–9.
- [3] Barakat S. *Housing reconstruction after conflict and disaster*. London: Overseas Development Institute; 2003.
- [4] Dodoo A, Gustavsson L. Life cycle primary energy use and carbon footprint of wood-frame conventional and passive houses with biomass-based energy supply. *Appl Energy* 2013;112:834–42.
- [5] Datin PL, Prevatt DO. Using instrumented small-scale models to study structural load paths in wood-framed buildings. *Eng Struct* 2013;54:47–56.
- [6] Imperadori M, Salvalai G, Pusceddu C. Air shelter house technology and its application to shelter units: the case of scaffold house and cardboard shelter installations. *Procedia Econ Finance* 2014;18:552–9.
- [7] Studzinski R, Pozorski Z, Garstecki A. Failure maps of sandwich panels with soft core, 10th international conference modern building materials, structures and techniques. p. 1060–5.
- [8] Lawson RM, Ogden RG. ‘Hybrid’ light steel panel and modular systems. *Thin Walled Struct* 2008;46:720–30.
- [9] Veljkovic M, Johansson B. Light steel framing for residential buildings. *Thin-Walled Struct* 2006;44:1272–9.
- [10] Winandy JE, Hunt JF, Turk C, Anderson JR. Emergency housing systems from three-dimensional engineered fiberboard: temporary building systems for lightweight, portable, easy-to-assemble, reusable, recyclable, and biodegradable structures, General Technical Report FPL-GTR-166. Madison, WI: U.S. Department of Agriculture, Forest Service, Forest Products Laboratory; 2006.
- [11] Sousa JM, Correia JR, Cabral-Fonseca S, Diogo AC. Effects of thermal cycles on the mechanical response of pultruded GFRP profiles used in civil engineering applications. *Compos Struct* 2014;116:720–31.
- [12] Correia JR, Cabral-Fonseca S, Branco FA, Ferreira JG, Eusébio MI, Rodrigues MP. Durability of pultruded glass-fiber-reinforced polyester profiles for structural applications. *Mech Compos Mater* 2006;42:325–38.

- [13] Rizkalla S, Lucier G, Dawood M. Innovative use of FRP for the precast concrete industry. *Adv Struct Eng* 2012;15:565–74.
- [14] Oppe MW, Knippers J. Application of bolted connections in fibre-reinforced polymers. *Proc Inst Civ Eng Struct Build* 2011;164:321–32.
- [15] Zenkert D. An introduction to sandwich construction. In: *Engineering materials advisory services*. Stockholm: Cradley Heath, Warley; 1995.
- [16] Vinson JR. The behavior of sandwich structures of isotropic and composite materials. United States of America: Technomic Publishing Company, Inc; 1999.
- [17] Kootsookos A, Burchill PJ. The effect of the degree of cure on the corrosion resistance of vinyl ester/glass fibre composites. *Compos A Appl Sci Manuf* 2004;35:501–8.
- [18] Nguyen CH, Chandrashekhara K, Birman V. Multifunctional thermal barrier coating in aerospace sandwich panels. *Mech Res Commun* 2012;39:35–43.
- [19] Allard JF, Atalla N. *Propagation of sound in porous media: modelling sound absorbing materials*, 2009.
- [20] Shawkat W, Honickman H, Fam A. Investigation of a novel composite cladding wall panel in flexure. *J Compos Mater* 2008;42:315–30.
- [21] Sharaf T, Shawkat W, Fam A. Structural performance of sandwich wall panels with different foam core densities in one-way bending. *J Compos Mater* 2010;44:2249–63.
- [22] Correia JR, Garrido M, Gonilha JA, Branco FA, Reis LG. GFRP sandwich panels with PU foam and PP honeycomb cores for civil engineering structural applications: effects of introducing strengthening ribs. *Int J Struct Integrity* 2012;3:127–47.
- [23] Keller T, Haas C, Vall'e T. Structural concept, design, and experimental verification of a glass fiber-reinforced polymer sandwich roof structure. *J Compos Constr* 2008;12:454–68.
- [24] Mousa MA, Uddin N. Global buckling of composite structural insulated wall panels. *Mater Des* 2011;32:766–72.
- [25] American Society for Testing and Materials. ASTM D3039/D3039M-14, standard test method for tensile properties of polymer matrix composite materials, 2000. West Conshohocken, PA 19428-2959, United States.

- [26] American Society for Testing and Materials. ASTM C365, standard test method for flatwise compressive properties of sandwich cores, 2005. West Conshohocken, PA 19428-2959, United States.
- [27] American Society for Testing and Materials. ASTM C273, standard test method for shear properties of sandwich core materials, 2000. West Conshohocken, PA 19428-2959, United States.
- [28] European Committee for Standardization (CEN). Eurocode 1: actions on structures – Part 1-1: general actions – densities, self-weight, imposed loads for buildings. Brussels: Technical Committee CEN/TC 250; 2002.
- [29] ASTM C393. Standard test method for flexural properties of sandwich constructions. West Conshohocken, PA 19428-2959: United States American Society for Testing and Materials; 2000.
- [30] Zenkert D, Shipsha A, Persson K. Static indentation and unloading response of sandwich beams. *Compos B Eng* 2004;35:511–22.
- [31] Petras A, Sutcliffe MPF. Indentation resistance of sandwich beams. *Compos Struct* 1999;46:413–24.
- [32] Rizov V, Shipsha A, Zenkert D. Indentation study of foam core sandwich composite panels. *Compos Struct* 2005;69:95–102.
- [33] Petras A, Sutcliffe MPF. Indentation failure analysis of sandwich beams. *Compos Struct* 2000;50:311–8.
- [34] Fam A, Sharaf T. Flexural performance of sandwich panels comprising polyurethane core and GFRP skins and ribs of various configurations. *Compos Struct* 2010;92:2927–35.
- [35] Russo A, Zuccarello B. Experimental and numerical evaluation of the mechanical behaviour of GFRP sandwich panels. *Compos Struct* 2007;81:575–86.
- [36] Carlsson LA, Kardomateas GA. Structural and failure mechanics of sandwich composites. New York: Springer; 2011.
- [37] Council INR. CNR, guide for the design and construction of structures made of FRP pultruded elements, 2008. Rome.